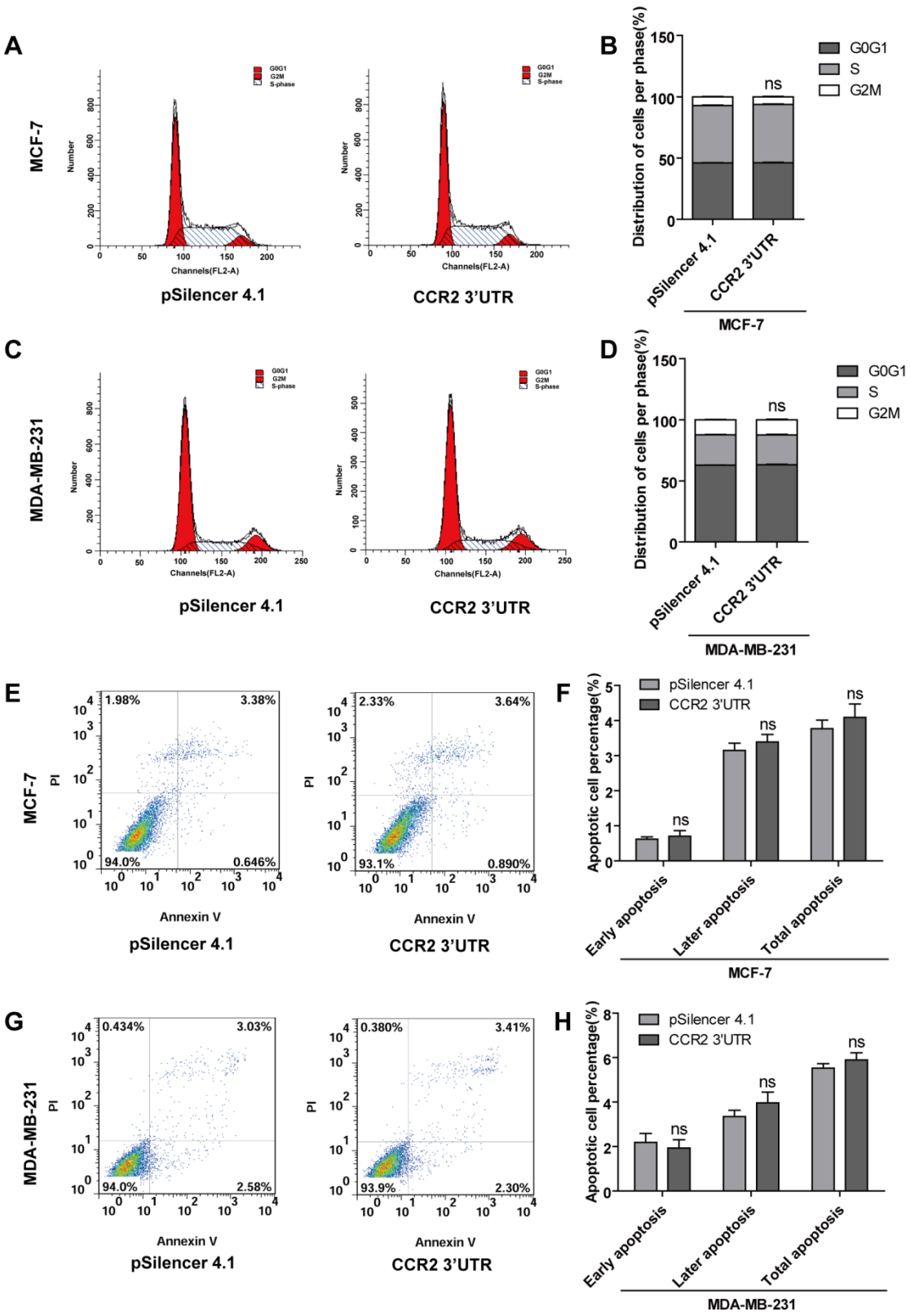


**Fig. S1. Flow cytometric detection of cell cycle and apoptosis of MCF-7 and MDA-MB-231 cells after transfection.** Cells were transfected with CCR2 3′UTR (pSilencer 4.1 harboring CCR2 3′UTR sequence) or control vector pSilencer 4.1 for 48h. (A and C) Cells were processed for flow cytometric analysis after PI staining and histograms showed cell distribution in G0/ G1, S and G2/

M phases of the cell cycle. (B and D) DNA content quantification in G0/ G1, S and G2/ M phases were shown. (E and G) Cells were stained with annexin V and PI. The numbers referred to the percentage of cells in upper right (later apoptosis) and lower right (early apoptosis) quadrants. (F) The changes of the early, the later and the total apoptotic percentages in transfected MCF-7 cells. (H) The changes of the early, the later and the total apoptotic percentages in transfected MDA-MB-231 cells. Data were presented as the mean ± SD, n =3, ns indicate no significant differences from control vector (pSilencer 4.1).

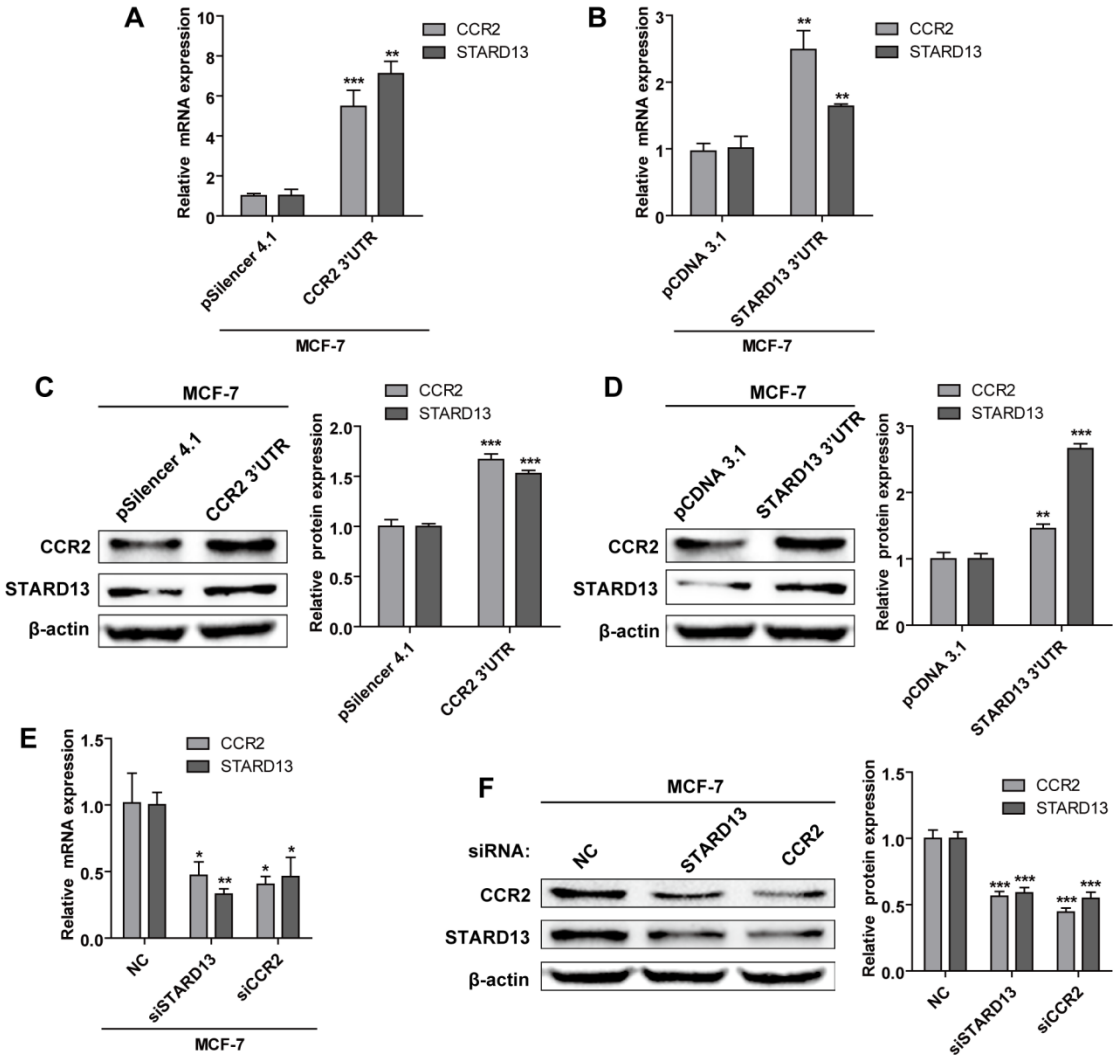


**Fig. S2. CCR2 3′UTR increases STARD13 expression and CCR2 knockdown decreases STARD13 expression.** (A and B) Overexpression of CCR2 3′UTR (A) or STARD13 3′UTR (B) increased CCR2 and STARD13 mRNA levels in MCF-7 cells, qRT-PCR analysis for expressions of CCR2 and STARD13. (C and D) Overexpression of CCR2 3′UTR (left panel of C) or STARD13 3′UTR (left panel of D) increased CCR2 and STARD13 protein levels in MCF-7 cells. Western analysis for CCR2 and STARD13 expressions and β-actin as a loading control was shown; (right panel of C and D) Quantification of CCR2 and STARD13 expressions. (E) STARD13 mRNA expression is efficiently reduced following treatment of MCF-7 cells with CCR2 siRNA, qRT-PCR analysis for expressions of CCR2 and STARD13. (F) CCR2 knockdown decreased STARD13 protein levels in MCF-7 cells (left panel of F). Western analysis for CCR2 and STARD13 expression and β-actin as a loading control was shown; (right panel of F) Quantification of CCR2 and STARD13 expressions. Data were presented as the mean ± SD, n =3, *p < 0.05, **p < 0.01, ***p < 0.001 vs. control vector.

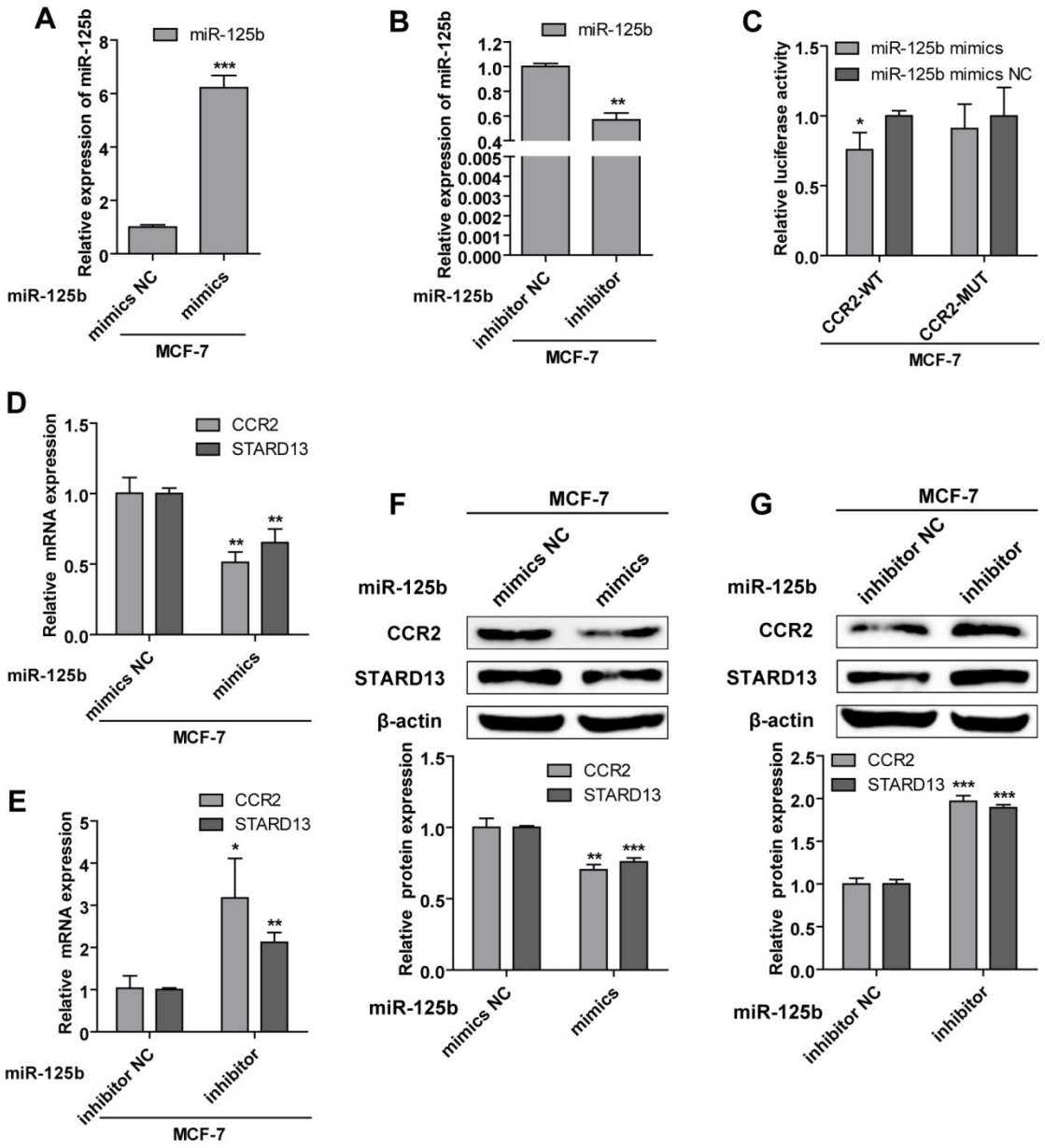


**Fig. S3. miR-125b regulates CCR2 and STARD13 expressions.** (A and B) The transfection efficiency of miR-125b mimics (A) and miR-125b inhibitor (B) was confirmed by qRT-PCR in MCF-7 cells. Data were presented as the mean ± SD, n =3, *p < 0.05, **p < 0.01, ***p < 0.001 vs. mimics NC or inhibitor NC. (C) After transfection, luciferase reporter assay confirmed the direct binding between miR-125b and CCR2 in MCF-7 cells. Luciferase activity in cells was measured and normalized to β-gal activity. Data were presented as the mean ± SD, n =3, *p < 0.05, **p < 0.01, ***p < 0.001 vs. mimics NC or inhibitor NC. (D) miR-125b mimics reduced mRNA levels of CCR2 and STARD13 in MCF-7 cells. (E) miR-125b inhibitor increased mRNA levels of CCR2 and STARD13 in MCF-7 cells. (F and G) Western analysis of CCR2 and STARD13 expressions in MCF-7 cells treated with miR-125b mimics (upper panel of F) or miR-125b inhibitor (upper panel of G), β-actin expression was shown as a loading control; (lower panel of F and G) Quantification of these proteins expressions. Data were presented as the mean ± SD, n =3, *p < 0.05, **p < 0.01, ***p < 0.001 vs. mimics NC or inhibitor NC.

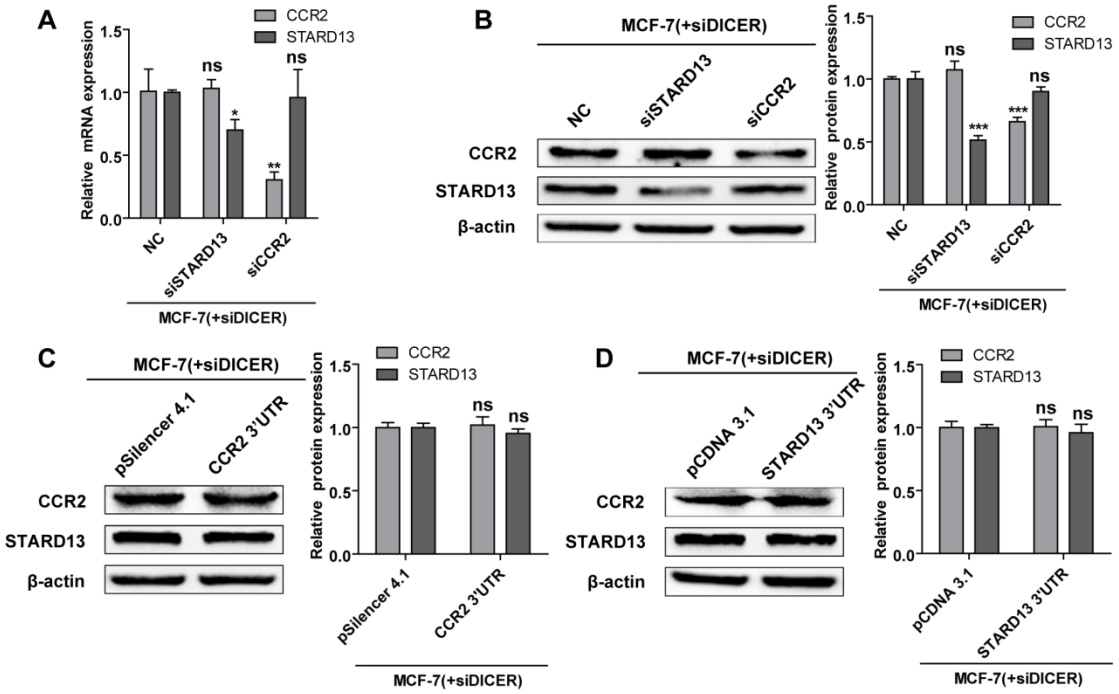


**Fig. S4. Regulation of STARD13 by CCR2 is microRNA dependent.** (A and B) When siCCR2 was co-transfected with siDICER, the mRNA (A) and protein (B) expressions of CCR2 and STARD13 were examined by qRT-PCR analysis. Data were presented as the mean ± SD, n =3, *p < 0.05, **p < 0.01, ***p < 0.001 vs. NC. (C and D) Western analyses were used to detect CCR2 and STARD13 protein expression in response to CCR2 3′UTR (left panel of C) and STARD13 3′UTR (left panel of D) overexpression in siDICER-treated MCF-7 cells; (right panel of C and D) Quantification of proteins expressions. Data were presented as the mean ± SD, n =3, *p < 0.05, **p < 0.01, ***p < 0.001 vs. control vector.

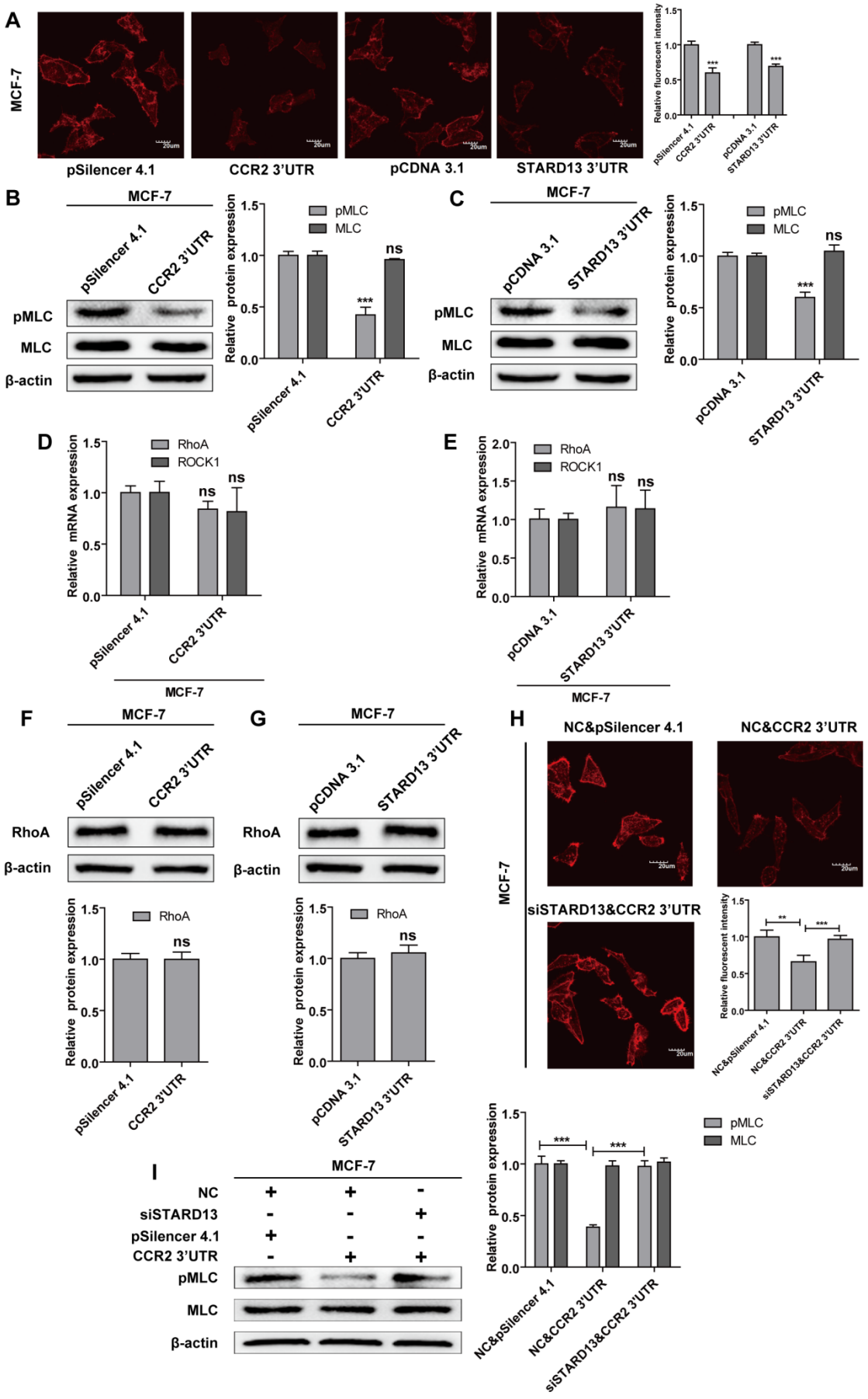

**Fig. S5. CCR2 3′UTR inhibits formation of F-actin stress fibers, RhoA activity and MLC phosphorylation.** (A) MCF-7 cells were stained with rhodamine-labeled phalloidin to detect F-actin stress fibers. Bars = 20 μm. (B and C) Western blot was used to detect $pMLC^{S19}$ protein in response to overexpression of CCR2 3′UTR (left panel of B) and STARD13 3′UTR (left panel of C) in MCF-7 cells; (right panel of B and C) Quantification of $pMLC^{S19}$ and MLC protein. (D and E) qRT-PCR was performed to quantify RhoA and ROCK1 mRNA levels in MCF-7 cells. (F and G) Western blot was performed to examine total RhoA protein level in response to overexpression of CCR2 3′UTR (upper panel of F) and STARD13 3′UTR (upper panel of G) in MCF-7 cells; (lower panel of F and G) Quantification of RhoA protein. Data were presented as the mean ± SD, n =3, *p < 0.05, **p < 0.01, *** p< 0.001 vs. control vector. ns indicate no significant differences from control vector (pSilencer 4.1 or pCDNA 3.1). (H) MCF-7 cells were transfected with siSTARD13 or NC in the presence or absence of overexpression CCR2 3′UTR and stained with rhodamine-labeled phalloidin. Immunofluorescence assay confirmed that siSTARD13 could reverse CCR2 3′UTR-induced inhibition of F-actin. Bars = 20 μm. (I) siSTARD13 reversed CCR2 3′UTR –induced down-regulation of phosphorylation of MLC protein in MCF-7 cells (left panel of I); (right panel of I) Quantification of $pMLC^{S19}$ and MLC protein. Data were presented as the mean ± SD, n =3, *p < 0.05, **p < 0.01, ***p < 0.001 vs. NC & pSilencer 4.1 or siSTARD13 & CCR2 3′UTR.

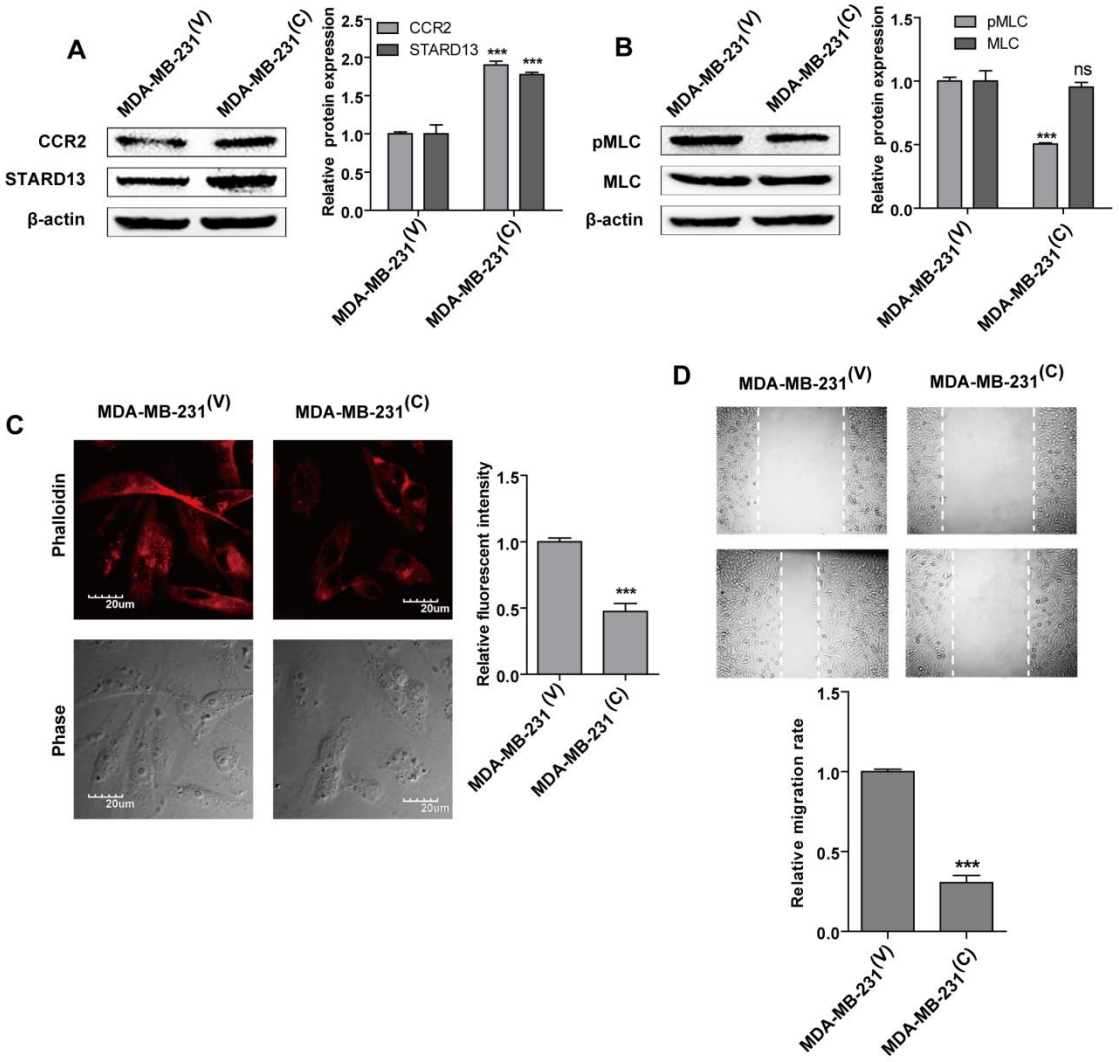


**Fig. S6. CCR2 3′UTR increases STARD13 expression and inhibits MLC phosphorylation, formation of stress fibers and migration of MDA-MB-231 cells.** (A) Western blot showed CCR2 and STARD13 protein in MDA-MB-231$^{(V)}$ cells (stably transfected with an empty vector) or MDA-MB-231$^{(C)}$ cells (stably transfected with CCR2 3′UTR) (left panel of A); (right panel of A) Quantification of CCR2 and STARD13 protein. (B) Western blot showed pMLC$^{S19}$ and MLC protein in MDA-MB-231$^{(V)}$ cells (stably transfected with an empty vector) or MDA-MB-231$^{(C)}$ cells (stably transfected with CCR2 3′UTR) (left panel of B); (right panel of B) Quantification of pMLC$^{S19}$ and MLC protein. (C) MDA-MB-231$^{(V)}$ cells and MDA-MB-231$^{(C)}$ cells were stained with rhodamine-labeled phalloidin to detect F-actin stress fibers. Phase contrast images were shown. Bars = 20 μm. (D) The cell motility rate was measured by wound healing assay, movement of cells into the wound was shown for MDA-MB-231$^{(V)}$ cells (stably transfected with an empty vector), MDA-MB-231$^{(C)}$ (stably transfected with CCR2 3′UTR). Data were presented as the mean ± SD, n =3, *p < 0.05, **p < 0.01, ***p < 0.001 vs. vector. ns indicate no significant differences from vector.

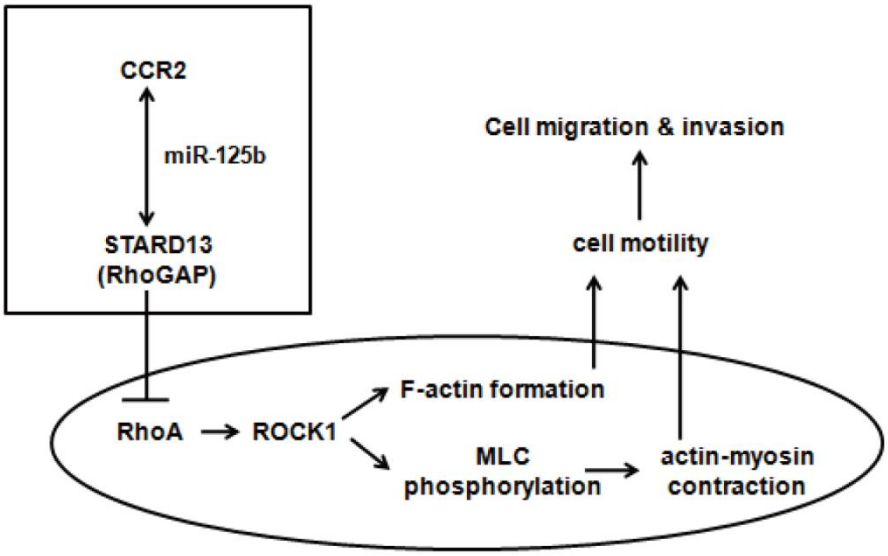


**Fig. S7. Proposed model for how CCR2 3′UTR through RhoA-ROCK1 signaling regulates motility of breast cancer cells.** CCR2 3′UTR regulates STARD13 expression through in a miR-125b-dependent manner. STARD13 inhibit RhoA-ROCK1 signaling activity through its RhoGAP domain, leading to inhibiting the RhoA-mediated assembly of actin stress fibers and MLC phosphorylation. The pathways converge to suppress cell motility, an essential step required for cell migration and invasion and cancer metastasis. Rectangle box: ceRNA crosstalk of CCR2, miRNA-125b and STARD13. Ovals box: RhoA-ROCK1 signaling pathway.